ACS Sustainable Chemistry & Engineering

Research Article

pubs.acs.org/journal/ascecg

Recovery of Volatile Fatty Acids from Fermented Wastewater by Adsorption

Ehsan Reyhanitash, Sascha R. A. Kersten, and Boelo Schuur*

Sustainable Process Technology Group, Faculty of Science and Technology, University of Twente, Drienerlolaan 5, Enschede 7522 NB, The Netherlands

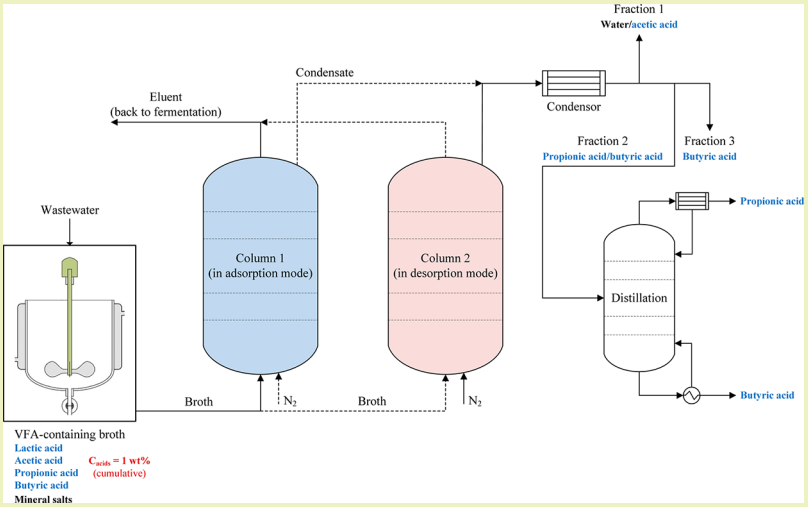

ABSTRACT: Separation of volatile fatty acids (VFAs) from fermented wastewater is challenging, due to low VFA concentrations in mineral-rich streams. As a result, separation capacity and selectivity with traditional solvents and adsorbents are both compromised. In this study, using a complex artificial model solution mimicking real fermented wastewaters, it is shown that a simple and robust adsorption-based separation technique can retain a remarkable capacity and selectivity for VFAs. Four types of polystyrene-divinylbenzene-based resins (primary, secondary, and tertiary amine-functionalized, and nonfunctionalized) were examined as the adsorbents. The presence of chloride, sulfate, and phosphate salts resulted in coadsorption of their acidic forms HCl, H_2SO_4, and H_3PO_4 on amine-functionalized adsorbents, and severely reduced the VFA capacity. With the nonfunctionalized adsorbent, almost no mineral acid coadsorption was observed. This together with a high total VFA capacity of up to 76 g/kg in equilibrium with the model solution containing a total VFA concentration of 1 wt % resulted in a very high selectivity for the VFAs. Nitrogen-stripping with various temperature profiles was applied to regenerate the adsorbent, and study the potential for fractionation of the VFAs during regeneration. Butyric acid (HBu) was obtained in mole fractions of up to 0.8 using a stepwise increase in the stripping temperature from 25 °C via 120 to 200 °C. During four successive adsorption−regeneration cycles, no reduction in the adsorption capacity was observed.

KEYWORDS: *Adsorption, Fractionation, Volatile fatty acids, Polystyrene-divinylbenzene, Fermented wastewater*

INTRODUCTION

Volatile fatty acids (VFAs) are widely used chemicals, and among other applications, they serve as precursors to fuels and high-value chemical products such as polymers.[1−4] The major fraction of the global VFA demand is met by the VFAs produced through petrochemical routes.[2] However, petroleum-based routes are considered unsustainable, and, therefore, recent research and development has aimed at cradle to cradle technologies such as biological production of VFAs from waste streams.[5−9] Using wastewater as fermentation feed produces broths with a much lower VFA content as compared to glucose-fed fermentation broths, due to the limited carbon content of wastewater. To achieve an economical production of biobased VFAs, implementation of a robust VFA recovery technique is inevitable. Furthermore, the presence of various ions in fermented wastewater in significant amounts must be considered when designing a downstream separation process. Na^+, K^+, $H_2PO_4^-/HPO_4^{2-}$, Cl^-, and SO_4^{2-} are the most common ions found in fermented wastewater (see Table 1 for the typical composition of fermented wastewater). Depending on the wastewater's origin and fermentation approach, the concentration of species may vary within the given ranges.

The acid content of a VFA-containing aqueous solution is a critical parameter to consider for choosing a suitable VFA

Received: June 26, 2017
Revised: September 1, 2017
Published: September 6, 2017

DOI: 10.1021/acssuschemeng.7b02095
ACS Sustainable Chem. Eng. 2017, 5, 9176−9184

Table 1. Typical Composition of Fermented Wastewater

component	chemical formula	concentration [g/L]	pK_a
acetic acid	CH_3COOH	2.5−10	4.76
propionic acid	CH_3CH_2COOH	2.5−10	4.88
butyric acid	$CH_3(CH_2)_2COOH$	2.5−10	4.82
lactic acid	$CH_3CH(OH)COOH$	2.5−10	3.86
sodium	Na^+	1−5	
potassium	K^+	1−5	
chloride	Cl^-	1−10	
phosphate	$H_2PO_4^-/HPO_4^{2-}$	1−10	
sulfate	SO_4^{2-}	1−10	
sulfide	S^{2-}	0.3	
magnesium	Mg^{2+}	0.3	
calcium	Ca^{2+}	0.3	
ammonium	NH_4^+	0.1	
trace elements (e.g., cobalt, nickel, and iron)	Co, Fe, Ni (ionic forms)	10^{-4}	
inert COD (e.g., humic acid and fulvic acid)		1	
microbes			

separation method.[10] Because water forms the majority of fermented wastewater, the chosen method has to target the VFA molecules and limit water removal as much as possible. To separate VFAs from highly dilute aqueous streams, an affinity agent is required. Selection and design of an affinity agent is an important element of studies toward effective VFA recovery by affinity separation. A strong affinity may lead to an effective VFA separation, but it makes recovering the VFAs from the affinity agent challenging. Both adsorption and liquid−liquid extraction have been examined as affinity separation methods for VFA recovery.[11−18] Adsorption enables separation of substances from dilute and complex solutions.[19] The effectiveness of adsorption is expressed with the term "capacity", which is often defined as the mass of adsorbate per kilogram of adsorbent. After performing adsorption, the adsorbate has to be desorbed from the adsorbent to complete the recovery process and regenerate the adsorbent. When adsorption is applied to a complex solution such as fermented wastewater, a high selectivity of the adsorbent for the compound of interest is essential.[20]

In the literature, various adsorbents have been proposed for adsorption of carboxylic acids.[12,17,21−28] Primary, secondary, and tertiary amines, and quaternary ammonium are the most common functional groups serving as reactive sites on these adsorbents. Quaternary ammonium-based adsorbents, also referred to as strongly basic adsorbents, are under normal fermentation conditions the only nitrogen-based adsorbents capable of recovering carboxylate anions through anion exchange.[23] The three amine forms can only adsorb carboxylic acids as charge-neutral units (either through hydrogen bonding or via proton transfer) to maintain the charge neutrality of the adsorbent phase. The pH of a VFA-containing fermented wastewater is typically 5−7, and, as a result, the VFAs are mostly in their dissociated forms. Although a quaternary ammonium-based adsorbent appears beneficial for carboxylate recovery from fermented wastewater, the ion exchange makes regeneration of the adsorbent impossible without another ion exchange with the mineral acid of the replaced anion of the ammonium.[25,29] This requires an extra chemical and processing stage, and, moreover, the VFA obtained after adsorbent regeneration is not pure, but in an aqueous solution containing a significant mineral impurity.

Therefore, in this study, the use of a quaternary ammonium-based adsorbent was omitted, and adsorption of VFAs from a complex model solution mimicking fermented wastewater (composition given in Table 1) was studied with polystyrene-divinylbenzene (PS-DVB) resins, which were either non-functionalized or functionalized with a primary, secondary, or tertiary amine. The equilibrium selectivities and capacities of the adsorbents were determined in batch experiments. The breakthrough curves, as well as the column loadings in equilibrium with feed, were obtained in a packed bed.

With regard to regeneration of the loaded adsorbents, a few desorption techniques have been reported in the literature. They involve performing a solvent wash to recover the adsorbed organic acids from the adsorbent.[12,24,25,29−33] The solvent can be water (or steam), an alkali solution, or an organic solvent (e.g., methanol). In all cases, the resulting stream has to be subjected to a post-treatment operation (e.g., distillation) to deliver a high-purity organic acid stream. In this study, direct desorption of the adsorbed VFAs by nitrogen-stripping was studied as an alternative regeneration method that, after condensation of the desorbed VFAs, may yield highly concentrated VFAs. A complete process including both adsorption and desorption stages for recovery of VFAs from fermented wastewater was proposed as well.

MATERIALS AND METHODS

Chemicals. Acetic acid (HAc, >99.7%), propionic acid (HPr, >99.5%), butyric acid (HBu, >99%), potassium chloride (>99%), anhydrous sodium phosphate dibasic (>99%), and anhydrous sodium sulfate (>99%) were purchased from Sigma-Aldrich. Crystalline lactic acid (HLa, >98%) was kindly provided by Corbion. Potassium hydroxide (1 M) was supplied by Merck. All of the adsorbents, Lewatit VP OC 1065 (primary amine), Amberlite IRA96 RF (secondary amine), Amberlite IRA96 SB (tertiary amine), and Lewatit VP OC 1064 MD PH (nonfunctionalized), were purchased from Lenntech. The water used was ultrapure (Milli-Q, with a resistance of 18.2 $\mu\Omega$ cm at 25 °C).

Model Solutions. Two main model solutions were prepared for this study: a model solution for fermented wastewater referred to as "feed", and a more concentrated form of feed referred to as "concentrate" in which the concentration of each species was 5 times that in feed. Table 2 shows the composition of the model solutions.

Next to feed and concentrate, several model solutions, referred to as concentrates, were prepared by diluting concentrate with water at

Table 2. Composition of Model Solution Representing Fermented Wastewater and Its Concentrated Variety

	concentration [wt %]				concentration [mol/L]			
solution	HAc[a]	HPr[b]	HBu[c]	HLa[d]	KCl	Na_2SO_4	Na_2HPO_4	pH
feed	0.25	0.25	0.25	0.25	0.05	0.05	0.1	4.98
concentrate	1.25	1.25	1.25	1.25	0.25	0.25	0.5	4.95

[a]Acetic acid. [b]Propionic acid. [c]Butyric acid. [d]Lactic acid.

DOI: 10.1021/acssuschemeng.7b02095
ACS Sustainable Chem. Eng. 2017, 5, 9176−9184

concentrate:water mass ratios of approximately 16:4, 13:8, 9:12, 4:16, and 1:90.

EXPERIMENTAL PROCEDURES

Batch Adsorbent Screening. To compare the capacities and selectivities of the adsorbents, feed concentrates (see Model Solutions) were used to construct competitive adsorption isotherms for the VFAs and minerals. A typical batch experiment was performed by contacting 1 g of an adsorbent (used as received, no pretreatment) with 21 g of a feed concentrate (both weighed on a balance with an accuracy of 0.0001 g) at room temperature (20 ± 1 °C). The exact mass of dry adsorbent was determined by correcting the initial value (~1 g) for the amount of moisture and preservatives. The mixtures were then stirred at >500 rpm for 1 h, which was sufficient to reach equilibrium. The equilibrium concentrations were measured with HPLC and IC, and the capacities were calculated on the basis of the differences between the initial and equilibrium contents. This method of preparing a multicomponent batch isotherm was adopted from an earlier study by Zhou et al.[34]

Capacity Determination in Column. To determine the actual capacity of an adsorbent in a column after a complete breakthrough (thus in equilibrium with feed), a glass column (d = 2.5 cm, l = 6 cm) was packed with the adsorbent as received. The adsorbent was then dried by flushing N_2 through the column at 120 °C for 3 h using the adsorbent regeneration mode of the setup depicted in Figure 1. The N_2 flow rate during the drying procedure was 0.2 L/min. Feed was then pumped through the column at room temperature (20 ± 1 °C) and 2 mL/min for >200 min, which was sufficient to saturate the column with feed. The column outlet was sampled periodically, and the samples were analyzed by HPLC and IC. The amount of each species retained by the column was calculated by closing a mass balance over the fed feed and the collected outlet samples. At the end of an adsorption experiment, before starting a desorption experiment, the column was flushed with N_2 at room temperature to drain a large fraction of feed from the dead volume of the column. The mass of drained feed was about twice the mass of feed remaining in the column afterward.

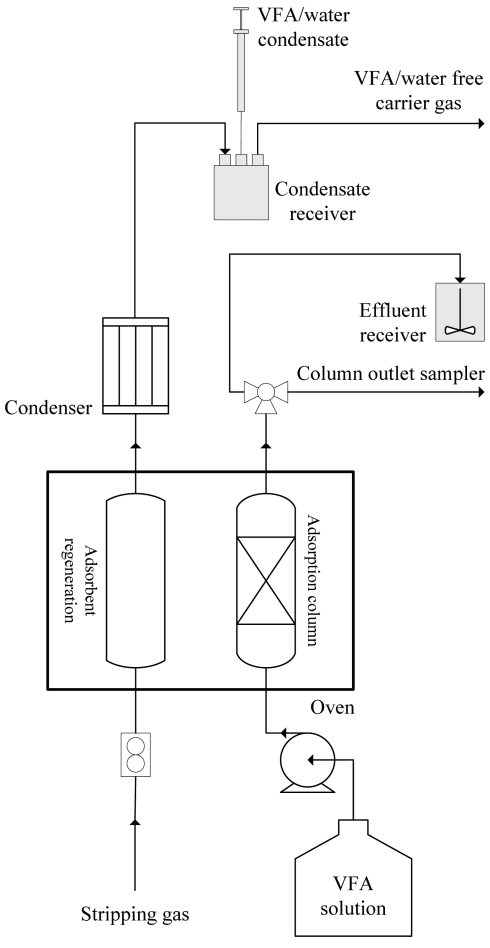

Figure 1. Schematic view of setup used for adsorbent drying, adsorption, and desorption. The condenser was operated at 5 °C with water as the cooling liquid.

Desorption Experiments. The desorption experiments were carried out by placing a weighed adsorption column containing an adsorbent in equilibrium with feed in the adsorbent regeneration section of the setup shown in Figure 1. Several temperature profiles were applied during desorption (see Table 3).

The stripping N_2 flow rate was always set at 0.2 L/min. After a desorption experiment was completed, the column was cooled to room temperature while the N_2 flow was on. After reaching room temperature, the N_2 flow was stopped, and the difference in the mass of the column before and after desorption (typically about 5 g) was used to assist with the mass balance over each species. For each temperature profile, several condensate samples were taken to determine the VFA concentration profile in the condensate over time. The condensate samples were analyzed by HPLC, representing evaporated species that were condensed in the condenser. It should be realized that not necessarily all of the acids evaporated during desorption, and, in addition, not all of the VFAs condensed totally in the condenser. The desorption experiment performed with temperature profile 3 was chosen as an example to assess the mass balance closure during desorption. The amount of the VFAs escaping the condensate receiver through the vapor phase (see Figure 1) was calculated using the UNIFAC-Pitzer model for vapor−liquid equilibria. To determine the VFA mass that remained inside the column after the desorption procedure was complete, an alkali-wash on a sample of the regenerated adsorbent was performed with a 1 M KOH solution at a KOH solution:adsorbent mass ratio of around 15:1. The obtained alkaline phases were then analyzed by HPLC for their VFA contents. A 1 M KOH solution:adsorbent mass ratio of 15:1 was sufficient for quantitative removal of the residual VFAs, as was experimentally validated with an additional wash.

Successive Adsorption−Desorption Cycles. To examine the stability of an adsorbent over the course of successive adsorption−desorption cycles, the adsorption/desorption procedures were performed consecutively to complete three cycles. The duration of desorption for each cycle was 3 h at a constant desorption temperature of 165, 180, or 200 °C. An additional set of four successive adsorption−desorption cycles in which a 15 min water-wash (2 mL/min) was applied on the saturated column before desorption at 165 °C was performed as well. Only for this set of experiments was a 1 h water-wash (2 mL/min) applied on the column containing fresh adsorbent before the first adsorption.

Analysis. The concentrations of HAc, HLa, HPr, HBu, and $H_3PO_4/H_2PO_4^-/HPO_4^{2-}/PO_4^{3-}$ were measured with HPLC [Agilent Hi-Plex H column (300 × 7.7 mm) using a refractive index detector on a Agilent 1200 series HPLC system; mobile phase, 5 mM H_2SO_4 solution; column temperature, 65 °C; flow rate, 0.6 mL/min]. Cl^- and SO_4^{2-} concentrations were quantified with ion chromatography (IC) (Metrosep A Supp 16-150/4.0 column on a Metrohm 850 Professional IC; mobile phase, 7.5 mM Na_2CO_3 + 0.75 mM KOH solution; column temperature, 45 °C; flow rate, 0.8 mL/min). Na^+ and K^+ concentrations were measured with IC as well (Metrosep C6-150/4.0 column on a Metrohm 850 Professional IC; mobile phase, 1.7 mM HNO_3 + 1.7 mM dipicolinic acid solution; column temperature, 20 ± 1 °C; flow rate, 1.0 mL/min). pH was measured with a Metrohm pH probe (6.0234.100) connected to a Metrohm 780 pH-meter.

RESULTS AND DISCUSSION

Batch Adsorbent Screening. In the batch adsorption experiments carried out with the feed concentrates, the initial VFA and salt concentrations were varied, but their ratio was

DOI: 10.1021/acssuschemeng.7b02095
ACS Sustainable Chem. Eng. 2017, 5, 9176−9184

Table 3. Temperature Profiles Applied for Adsorption

	time period 1		time period 2		time period 3	
temp profile no.	duration [min]	temp [°C]	duration [min]	temp [°C]	duration [min]	temp [°C]
1	60	180 ± 1				
2	30	120 ± 1	50	180 ± 1		
3	180	20 ± 1	60	120 ± 1	40	200 ± 1

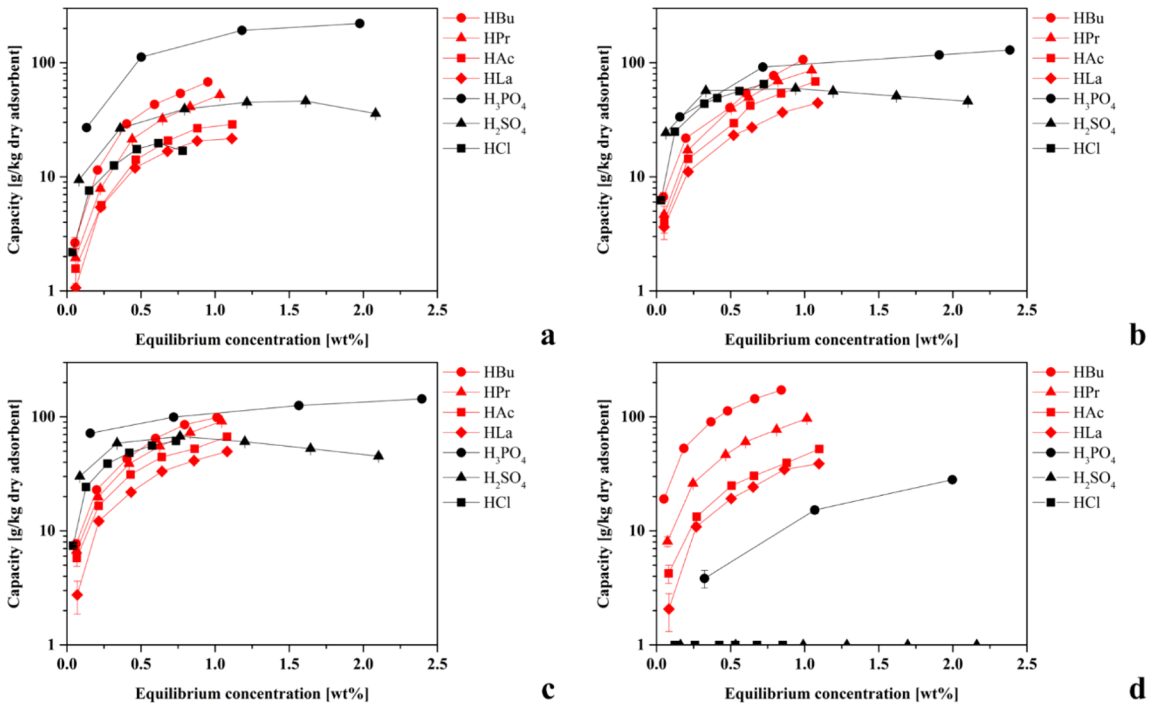

Figure 2. Multicomponent competitive batch adsorption isotherms obtained with (a) Lewatit VP OC 1065 (primary amine), (b) Amberlite IRA96 RF (secondary amine), (c) Amberlite IRA96 SB (tertiary amine), and (d) Lewatit VP OC 1064 MD PH (nonfunctionalized), T = 20 ± 1 °C. Equilibrium concentrations of multivalent species represent the summation of the concentrations of all forms of that species present in the sample. The initial pH of the aqueous solutions was approximately 5.

Table 4. Analysis of Aqueous Phases Obtained after Batch Adsorption Experiments for Na^+ and K^+

	Lewatit VP OC 1065 (primary amine)		Amberlite IRA96 RF (secondary amine)		Amberlite IRA96 SB (tertiary amine)		Lewatit VP OC 1064 MD PH (nonfunctionalized)		
batch adsorption with concentrate:feed (cation)	mass before [g]	mass after [g]	mass before [g]	mass after [g]	mass before [g]	mass after [g]	mass before [g]	mass after [g]	error [g]
16:4 (Na^+)	0.514	0.517	0.511	0.520	0.501	0.505	0.509	0.519	±0.005
16:4 (K^+)	0.147	0.148	0.146	0.148	0.142	0.143	0.144	0.144	±0.002
4:16 (Na^+)	0.132	0.138	0.132	0.136	0.128	0.133	0.156	0.166	±0.002
4:16 (K^+)	0.038	0.039	0.038	0.038	0.036	0.038	0.044	0.044	±0.001

kept the same. The obtained capacities with the four adsorbents for all of the species as a function of their equilibrium aqueous phase concentrations are displayed in Figure 2a–d. Although the analysis error was smaller than 1%, an analysis error of 1% was taken into account to calculate the error in the capacities, which was typically less than 5%, as reflected in the small error bars in Figure 2.

The analysis of the aqueous phases obtained after adsorption showed that neither Na^+ nor K^+ was adsorbed by any of the adsorbents (see Table 4), which implies that the adsorbed mineral anions must have been adsorbed together with H^+ to obey the charge neutrality constraint. This implies that the deprotonation equilibria of the VFAs shifted, and the remaining VFAs in the aqueous phases were mostly present as carboxylate salts. The chloride, sulfate, and phosphate loadings on the amine-functionalized adsorbents were very high, even exceeding capacities of 200 g/kg dry adsorbent for H_3PO_4. Their capacity for H_2SO_4 was somewhat lower, slightly decreasing with increasing aqueous concentration after reaching a maximum of about 70 g/kg dry adsorbent, likely due to competitive adsorption. Competitive adsorption similarly affected the HCl isotherm obtained with the primary amine-based adsorbent. The major drawback of mineral acid coadsorption was the remarkably lower capacity of the amine-based adsorbents for the VFAs. The mineral acid coadsorption by the amine-based adsorbents was in fact so large that using idealized model solutions solely containing the VFAs may well lead to completely different findings.[30,35] Besides losing capacity for the VFAs, mineral acid coadsorption may result in problematic adsorbent regeneration, and, if not removed, the

DOI: 10.1021/acssuschemeng.7b02095
ACS Sustainable Chem. Eng. 2017, 5, 9176–9184

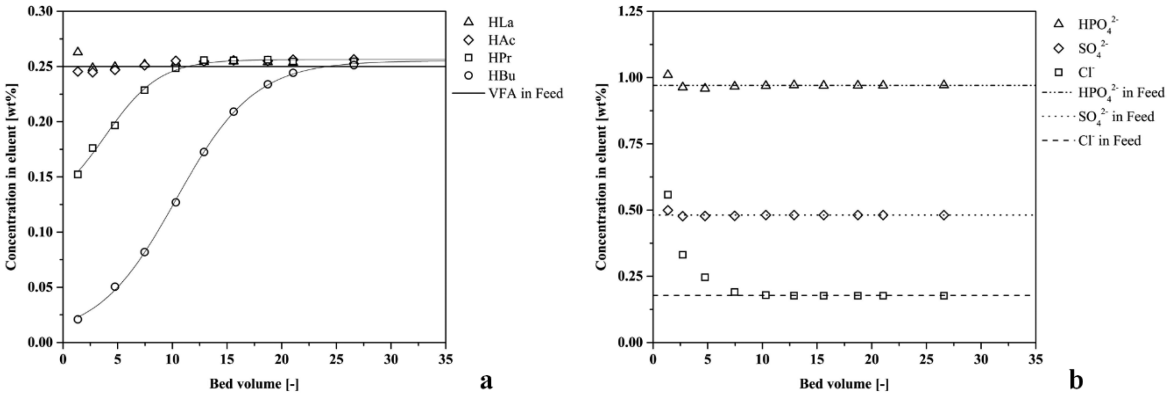

Figure 3. Breakthrough curves for VFAs (a) and mineral acids (b) using an adsorption column packed with 6.15 g of nonfunctionalized adsorbent. Feed flow rate: 2 mL/min, $T = 20 \pm 1$ °C.

mineral acids may accumulate on the adsorbent over time leading to a reduced adsorbent lifetime. Figure 2 also shows that the primary amine-based adsorbent has the highest H_3PO_4 capacity, which implies that it might be a potential phosphate recovery agent in the presence of a H^+ source.

As can be seen in Figure 2, the highest VFA capacities were achieved with the nonfunctionalized adsorbent (Figure 2d). The VFA molecules interact with the nonfunctionalized adsorbent through the hydrogen bond−π interactions between their carboxyl groups and the adsorbent's aromatic rings, and the hydrophobic interactions between the hydrocarbon chain and the adsorbent surface. With an increase in the length of the hydrocarbon chain, the hydrophobic section of the VFA molecule becomes larger resulting in a favored adsorption. A similar trend was previously observed with extraction of VFAs using physical (noncomplexing) solvents.[36] This behavior was observed for the amine-based adsorbents in Figure 2 as well, which may be explained by the amine-based adsorbents sharing the same hydrophobic polymer matrix of the nonfunctionalized adsorbent, and thus having a similar hydrophobic interaction with the hydrocarbon chain. No measurable capacity for the strong acids H_2SO_4 and HCl was observed with the nonfunctionalized adsorbent, as they were fully dissociated. For the weaker mineral acid H_3PO_4, a limited adsorption capacity was observed, which can be explained with its dissociation equilibrium enabling some undissociated H_3PO_4 to adsorb. Where the interaction of the strong mineral acids with amines is supported through ion-pair formation with the lone pair of nitrogen,[37] the nonfunctionalized adsorbent lacking these nitrogen lone pairs does not adsorb any strong mineral acid.

The high selectivity of the nonfunctionalized adsorbent for the VFAs makes it the most promising candidate for VFA separation from a VFA-containing fermented wastewater, and, therefore, further studies were carried out with this adsorbent.

Capacity Determination in Column. The concentration profile of the eluent leaving the column packed with the nonfunctionalized adsorbent is shown in Figure 3.

As can be seen in Figure 3, after about 22 bed volumes, the column was saturated with all of the adsorbates. A fast breakthrough was observed for HAc, as the adsorbent capacity for it was very limited (see Figure 3a and Table 5). The breakthroughs of HPr and HBu were slower due to the higher capacity of the adsorbent for them (see Figure 3a and Table 5). The sudden and significant drop in Cl^- concentration is an indication of the presence of Cl^- in the fresh adsorbent (Figure 3b). The aqueous solutions obtained after the batch adsorption experiments with the nonfunctionalized adsorbent contained extra Cl^- as well, and as indicated by the extra amounts of Na^+ in Table 4, Na^+ was the counterion. HLa, SO_4^{2-}, and HPO_4^{2-} left the column with almost no interaction with the adsorbent. The capacities reported in Table 5 have been determined five times under identical conditions, and the reported error in Table 5 is the standard deviation of these five results.

Table 5. Capacities Determined after Complete Breakthrough in Column ($T = 20 \pm 1$ °C) As Compared To Batch Adsorption Capacities

adsorbed compound	column capacity [g/kg adsorbent, ±3.5%]	batch capacity[a] [g/kg adsorbent]
HLa	0.0	9.7
HAc	1.5	12.5
HPr	13.3	26.5
HBu	60.7	65.2
H_3PO_4	0.0	13.4
H_2SO_4	0.0	0.0
HCl	0.0	0.0

[a]Derived from Figure 4.

Because of the complexity of the aqueous solutions used in the batch experiments, and the competitive nature of multicomponent adsorption, the equilibrium aqueous concentrations varied from those in feed. In the batch experiment that resulted in the equilibrium VFA concentrations closest to those in feed (indicated with open symbols in Figure 4, a magnified view of Figure 2d), the corresponding mineral content was higher than that in feed. This induced a salting-out effect resulting in VFA capacities higher than those obtainable in a column experiment.[38,39] The capacities obtained with this batch experiment are compared to those obtained with a column experiment in Table 5. Although the absolute values of the adsorption capacities obtained in the column experiment varied from those obtained with the batch experiment, the conclusions regarding capacity and selectivity for the VFAs remained unchanged.

Adsorbent Regeneration. To produce concentrated VFA streams, performing a water- or strong alkali-wash on the adsorbent is not suitable, as the resulting stream will either have a large water content or contain carboxylate salts rather than free VFAs.[24,25,29−32] Therefore, adsorbent regeneration methods that involve a thermal operation have been investigated instead.[12,40−42]

DOI: 10.1021/acssuschemeng.7b02095
ACS Sustainable Chem. Eng. 2017, 5, 9176−9184

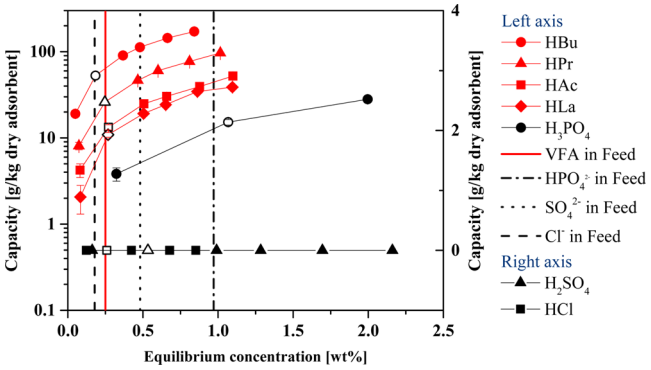

Figure 4. Batch experiments with nonfunctionalized adsorbent. The figure is similar to Figure 2d. It now indicates deviation of the equilibrium concentrations (open symbols) from the concentrations in feed.

In the first desorption experiment (temperature profile 1, see Table 3), a saturated column (in equilibrium with feed) was heated to 180 °C while being flushed with N_2 (at 0.2 L/min) for 1 h to investigate the feasibility of thermal regeneration. The VFA concentration profiles in the condensate in time are displayed in Figure 5.

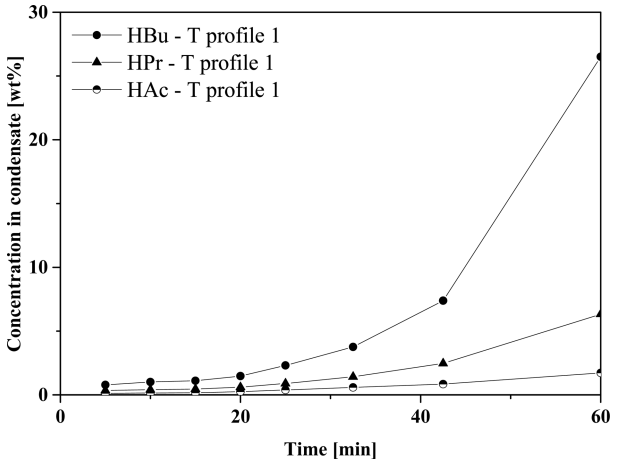

Figure 5. Condensate concentration profile in time by applying temperature profile 1. 6.15 g Adsorbent in column; the N_2 flow rate was 0.2 L/min.

As can be clearly seen in Figure 5, HPr and HBu concentrations increased simultaneously in time, following the same order seen in their column capacities and reaching a cumulative concentration of about 33 wt %. Considering that their cumulative concentration in feed was only 0.50 wt %, the VFA concentration in the condensate exhibited a strong increase. The limited capacity of the adsorbent for HAc limited its concentration in the condensate. Integrated over time, the VFA concentration in the condensate amounted approximately 10 wt %. Thus, the selective adsorption of the VFAs led to a significant increase in the VFA concentration. The majority of the water was not adsorbed on the surface of the pores, but remained in the liquid phase inside the pores of the adsorbent. The continuous rise in the VFA concentrations during desorption was due to a faster evaporation of the nonadsorbed pore-water and its lower boiling point. This corresponds to a gradual temperature rise inside the column to eventually reach the set point of 180 °C. After 60 min, no condensate was collected anymore, indicating that all of the water and VFAs evaporated from the column, and, therefore, the desorption procedure was stopped. A KOH-wash was then performed on a sample of the regenerated adsorbent to determine the residual adsorbate amounts in the column, and hence examine desorption efficiency. The obtained results are shown in Table 6.

Table 6. Condensate Composition To Be Obtained by Complete Condensation of Vapors after Applying Temperature Profile No. 1 on Lewatit VP OC 1064 MD PH (Nonfunctionalized Adsorbent)

species in feed	species on adsorbent and in condensate	loading on adsorbent prior to desorption [g/kg dry adsorbent]	cumulative concentration of all possible forms[a] [wt %]		percentage desorbed[b] [%]
			feed	condensate	
HLa/La^-	HLa	0.0	0.25	0.00	
HAc/Ac^-	HAc	1.5	0.25	0.45	100
HPr/Pr^-	HPr	13.3	0.25	1.77	100
HBu/Bu^-	HBu	60.7	0.25	7.27	99
PO_4^{3-}/ HPO_4^{2-}/ $H_2PO_4^-$/ H_3PO_4	H_3PO_4	0.0	0.96	0.00	
SO_4^{2-}/ HSO_4^-/ H_2SO_4	H_2SO_4	0.0	0.48	0.00	
Cl^-/HCl	HCl	0.0	0.18	0.00	
water	water (in pores)	926.9	96.47	90.50	100

[a]Assuming all of the VFAs and water desorbed by applying temperature profile 1 are condensed to form a single condensate. [b]Determined by performing a KOH-wash on the adsorbent after desorption.

As can be seen in Table 6, desorption using temperature profile 1 provides a significant purification step by which the total VFA concentration increases from 1 to around 10 wt %, and the obtained condensate is solely composed of water, HAc, HPr, and HBu, and it is essentially free of minerals. The adsorbed HAc, HPr, and HBu were completely recovered from the adsorbent. The easy and complete thermal removal of the adsorbed VFAs from the nonfunctionalized adsorbent is an indication of the weak nature of the adsorbent−VFA interaction.

To isolate considerable fractions of the adsorbed VFAs in higher concentrations in the condensate, the use of temperature profiles with additional temperature increments for desorption was studied. By applying temperature profile 2, a significant amount of the water was evaporated at 120 °C in the first 30 min, while the VFA concentrations in the condensate stayed minimal. After 30 min, the temperature was raised to 180 °C to completely desorb the VFA-rich fraction. To examine the possibility of removing a fraction of the water at room temperature and improving the VFA-rich fraction of the condensate, temperature profile 3 was applied. Figure 6 shows the VFA concentration profile of the condensate obtained with temperature profiles 2 and 3.

As can be seen in Figure 6, significantly higher VFA concentrations of up to 83.7% for HBu were obtained by applying temperature profile 2. Temperature profile 3 boosted

DOI: 10.1021/acssuschemeng.7b02095
ACS Sustainable Chem. Eng. 2017, 5, 9176−9184

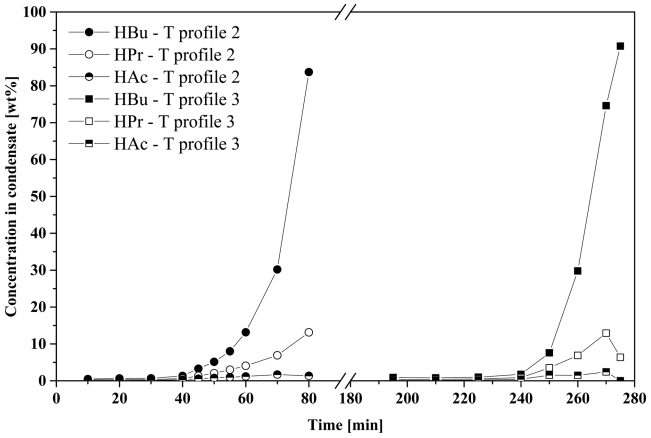

Figure 6. Condensate concentration profile in time by applying temperature profiles 2 or 3. 5.91 g Adsorbent in column for temperature profile 2; for temperature profile 3 this was 5.76 g adsorbent; N_2 flow rate was 0.2 L/min.

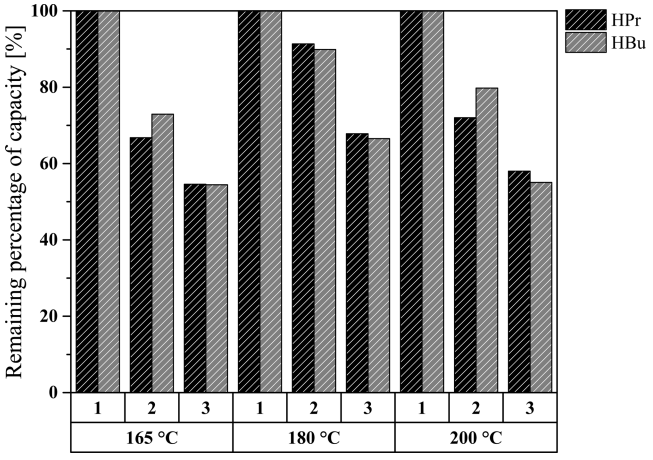

Figure 7. Capacity percentage retained on nonfunctionalized adsorbent over three successive adsorption−desorption cycles with a desorption temperature of 165, 180, or 200 °C.

the VFA concentration profile in the condensate even further. During the first 180 min, no condensate was collected. However, measuring the mass of the column after 180 min indicated a significant mass loss, and if all associated with water, it accounted for around 10 wt % of the initial water mass. The HAc and HPr concentrations in the condensate peaked at 270 min, whereas the HBu concentration continuously increased in time. This implies that, with a proper temperature profile, it may be possible to fractionate the VFAs during desorption. An additional stationary temperature step between the boiling points of HPr and HBu and a proper column design can further improve fractionation of the VFA-rich fraction.

The mass balance over desorption while applying temperature profile 3 resulted in 93.5% closure for HBu and 89.7% closure for HPr, which is acceptable considering the vapor phase above the collected condensate was approximated with a VLE model.

On the basis of the results presented so far, it can be concluded that a single adsorption−desorption cycle in which the high temperature exposure duration of the adsorbent is <50 min (50 min for temperature profile 2 and 40 min for temperature profile 3) is promising for VFA recovery from a VFA-containing fermented wastewater.

Adsorbent Life Cycle Assessment. To further assess the performance and stability of the adsorbent over several cycles of use, three series of three adsorption−desorption cycles were performed with desorption at 165, 180, or 200 °C for 3 h. The capacities were calculated with the procedure previously described. The obtained results are depicted in Figure 7.

As can be seen in Figure 7, the adsorbent lost a significant part of its capacity after each adsorption−desorption cycle. A similar behavior is often observed for other adsorbents reported in the literature.[25,43] However, Figure 7 also suggests that there is no correlation between capacity loss and temperature, and, therefore, thermal degradation of the adsorbent was most likely not the reason behind the capacity loss. A potential reason for capacity loss could be deposition of the salts inside the pores of the adsorbent. During adsorption, the salts enter the pores without being adsorbed, and upon evaporation of water and the VFAs, they deposit inside the pores blocking the sites for the VFA in the next cycle. To verify this hypothesis, an additional set of adsorption−desorption cycles was performed with a water-wash stage prior to desorption at 165 °C. The results are depicted in Figure 8.

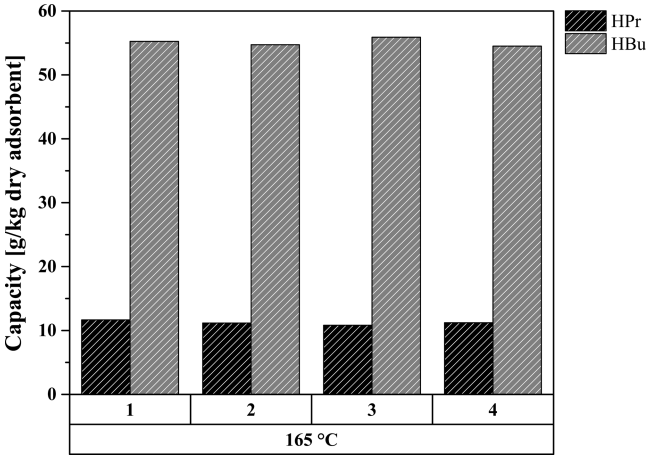

Figure 8. Capacity of nonfunctionalized adsorbent during four successive adsorption−desorption cycles with water-wash and a desorption temperature of 165 °C.

Figure 8 shows that indeed short water-wash stages between adsorption−desorption cycles stopped capacity loss. However, during a water-wash stage that took about 15 min, approximately 5 wt % of the adsorbed HBu and 20 wt % of the adsorbed HPr were removed from the column. Optimization of the water-wash stages can reduce the VFA losses without compromising the stability. As the VFA removal from the column by water was almost linear with time (at a constant water flow), shortening the duration of a water-wash stage by more than a factor of 2 to 6 min, just enough to fill the column, appears well possible. The stable performance over four adsorption−desorption cycles indicating the potential for an extensive operation, high selectivity, and low price (about 15 euro/$L_{adsorbent}$, bulk price) make the nonfunctionalized adsorbent ideal for VFA recovery from highly diluted and complex aqueous streams such as fermented wastewater. The adsorbent did not exhibit any capacity loss over four adsorption−desorption cycles, which is an indication of no adsorbent loss. This is clearly an advantage for this process as compared to liquid−liquid extraction-based processes where

DOI: 10.1021/acssuschemeng.7b02095
ACS Sustainable Chem. Eng. 2017, 5, 9176−9184

entrainment always causes small solvent losses and raffinate impurities.

CONCLUSIONS

Adsorption of volatile fatty acids (VFAs) from a complex solution mimicking fermented wastewater was studied using amine-functionalized polystyrene-divinylbenzene-based (PSDVB) resins as well as a nonfunctionalized PSDVB resin. The nonfunctionalized resin showed a very high selectivity for VFAs, while the amine-functionalized resins adsorbed mineral acids preferentially. Regeneration of the nonfunctionalized resin with a short water-wash stage followed by a temperature-profiled evaporation enabled fractionation of VFAs, and butyric acid was obtained with purities of up to 91 wt % (starting with a feed concentration of only 0.25 wt %). The nonfunctionalized resin proved very stable over four adsorption−desorption cycles, each of which included a short water-wash stage between adsorption and desorption stages. Overall, the nonfunctionalized resin utilized in the proposed adsorption−desorption process can deliver high-purity biobased VFA streams in a sustainable manner, without any risk of solvent leaching associated with liquid−liquid extraction-based processes.

AUTHOR INFORMATION

Corresponding Author

*Phone: +31 53 489 2891. E-mail: b.schuur@utwente.nl.

ORCID

Boelo Schuur: 0000-0001-5169-4311

Notes

The authors declare no competing financial interest.

ACKNOWLEDGMENTS

We acknowledge the financial support by NWO-TTW and Paques through the NWO-TTW Paques Program.

REFERENCES

(1) Agreda, V. H. *Acetic Acid and its Derivatives*; Taylor & Francis: UK, 1992.

(2) Straathof, A. J. J. Transformation of Biomass into Commodity Chemicals Using Enzymes or Cells. *Chem. Rev.* **2014**, *114* (3), 1871−1908.

(3) Lange, J.-P.; Price, R.; Ayoub, P. M.; Louis, J.; Petrus, L.; Clarke, L.; Gosselink, H. Valeric Biofuels: A Platform of Cellulosic Transportation Fuels. *Angew. Chem., Int. Ed.* **2010**, *49* (26), 4479−4483.

(4) Bond, J. Q.; Alonso, D. M.; Wang, D.; West, R. M.; Dumesic, J. A. Integrated Catalytic Conversion of γ-Valerolactone to Liquid Alkenes for Transportation Fuels. *Science* **2010**, *327* (5969), 1110−1114.

(5) McDonough, W.; Braungart, M. *Cradle to Cradle: Remaking the Way We Make Things*; Farrar, Straus, and Giroux: 2010.

(6) Lee, W. S.; Chua, A. S. M.; Yeoh, H. K.; Ngoh, G. C. A review of the production and applications of waste-derived volatile fatty acids. *Chem. Eng. J.* **2014**, *235* (0), 83−99.

(7) Blasig, J. D.; Holtzapple, M. T.; Dale, B. E.; Engler, C. R.; Byers, F. M. Volatile fatty acid fermentation of AFEX-treated bagasse and newspaper by rumen microorganisms. *Resour. Conserv. Recycl.* **1992**, *7* (1−3), 95−114.

(8) Sans, C.; Mata-Alvarez, J.; Cecchi, F.; Pavan, P.; Bassetti, A. Volatile fatty acids production by mesophilic fermentation of mechanically-sorted urban organic wastes in a plug-flow reactor. *Bioresour. Technol.* **1995**, *51* (1), 89−96.

(9) Dahiya, S.; Sarkar, O.; Swamy, Y. V.; Venkata Mohan, S. Acidogenic fermentation of food waste for volatile fatty acid production with co-generation of biohydrogen. *Bioresour. Technol.* **2015**, *182* (0), 103−113.

(10) Drake, B. D.; Howell, C. J.; Chen, P. N.; Wakefield, A. High boiling solvent system for recovery of acetic acid from aqueous solutions. EU Patent 0134650A1, 1985.

(11) López-Garzón, C. S.; Straathof, A. J. J. Recovery of carboxylic acids produced by fermentation. *Biotechnol. Adv.* **2014**, *32* (5), 873−904.

(12) Garcia, A. A.; King, C. J. The use of basic polymer sorbents for the recovery of acetic acid from dilute aqueous solution. *Ind. Eng. Chem. Res.* **1989**, *28* (2), 204−212.

(13) Wasewar, K. L.; Yawalkar, A. A.; Moulijn, J. A.; Pangarkar, V. G. Fermentation of Glucose to Lactic Acid Coupled with Reactive Extraction: A Review. *Ind. Eng. Chem. Res.* **2004**, *43* (19), 5969−5982.

(14) Reyhanitash, E.; Zaalberg, B.; Kersten, S. R. A.; Schuur, B. Extraction of volatile fatty acids from fermented wastewater. *Sep. Purif. Technol.* **2016**, *161*, 61−68.

(15) Blahušiak, M.; Schlosser, Š.; Marták, J. Extraction of butyric acid with a solvent containing ammonium ionic liquid. *Sep. Purif. Technol.* **2013**, *119*, 102−111.

(16) Tonova, K.; Svinyarov, I.; Bogdanov, M. G. Hydrophobic 3-alkyl-1-methylimidazolium saccharinates as extractants for l-lactic acid recovery. *Sep. Purif. Technol.* **2014**, *125* (0), 239−246.

(17) Thang, V. H.; Novalin, S. Green Biorefinery: Separation of lactic acid from grass silage juice by chromatography using neutral polymeric resin. *Bioresour. Technol.* **2008**, *99* (10), 4368−4379.

(18) Reyhanitash, E.; Zaalberg, B.; Ijmker, H. M.; Kersten, S. R. A.; Schuur, B. CO2-enhanced extraction of acetic acid from fermented wastewater. *Green Chem.* **2015**, *17* (8), 4393−4400.

(19) Ijmker, H. M.; Gramblička, M.; Kersten, S. R. A.; van der Ham, A. G. J.; Schuur, B. Acetic acid extraction from aqueous solutions using fatty acids. *Sep. Purif. Technol.* **2014**, *125* (0), 256−263.

(20) Joglekar, H. G.; Rahman, I.; Babu, S.; Kulkarni, B. D.; Joshi, A. Comparative assessment of downstream processing options for lactic acid. *Sep. Purif. Technol.* **2006**, *52* (1), 1−17.

(21) Kawabata, N.; Yoshida, J.-i.; Tanigawa, Y. Removal and recovery of organic pollutants from aquatic environment. 4. Separation of carboxylic acids from aqueous solution using crosslinked poly(4-vinylpyridine). *Ind. Eng. Chem. Prod. Res. Dev.* **1981**, *20* (2), 386−390.

(22) Keil, K. H.; Greiner, U.; Engelhardt, F.; Kuhlein, K.; Keller, R.; Schlingmann, M. Copolymer, a process for its preparation and its use as a sorbent. U.S. Patent 4552905, 1985.

(23) Tung, L. A.; King, C. J. Sorption and extraction of lactic and succinic acids at pH > pKa1. I. Factors governing equilibria. *Ind. Eng. Chem. Res.* **1994**, *33* (12), 3217−3223.

(24) Davison, B. H.; Nghiem, N. P.; Richardson, G. L. Succinic acid adsorption from fermentation broth and regeneration. *Appl. Biochem. Biotechnol.* **2004**, *114* (1), 653−669.

(25) Aljundi, I. H.; Belovich, J. M.; Talu, O. Adsorption of lactic acid from fermentation broth and aqueous solutions on Zeolite molecular sieves. *Chem. Eng. Sci.* **2005**, *60* (18), 5004−5009.

(26) Batault, F.; Thevenet, F.; Hequet, V.; Rillard, C.; Le Coq, L.; Locoge, N. Acetaldehyde and acetic acid adsorption on TiO2 under dry and humid conditions. *Chem. Eng. J.* **2015**, *264*, 197−210.

(27) Cano, M.; Sbargoud, K.; Allard, E.; Larpent, C. Magnetic separation of fatty acids with iron oxide nanoparticles and application to extractive deacidification of vegetable oils. *Green Chem.* **2012**, *14* (6), 1786−1795.

(28) Song, M.; Jiao, P.; Qin, T.; Jiang, K.; Zhou, J.; Zhuang, W.; Chen, Y.; Liu, D.; Zhu, C.; Chen, X.; Ying, H.; Wu, J. Recovery of lactic acid from the pretreated fermentation broth based on a novel hyper-cross-linked meso-micropore resin: Modeling. *Bioresour. Technol.* **2017**, *241*, 593−602.

(29) Wang, C.; Li, Q.; Wang, D.; Xing, J. Improving the lactic acid production of Actinobacillus succinogenes by using a novel fermentation and separation integration system. *Process Biochem.* **2014**, *49* (8), 1245−1250.

DOI: 10.1021/acssuschemeng.7b02095
ACS Sustainable Chem. Eng. 2017, 5, 9176−9184

(30) Cao, X.; Yun, H. S.; Koo, Y.-M. Recovery of l-(+)-lactic acid by anion exchange resin Amberlite IRA-400. *Biochem. Eng. J.* **2002**, *11* (2−3), 189−196.
(31) Evangelista, R. L.; Nikolov, Z. L. Recovery and purification of lactic acid from fermentation broth by adsorption. *Appl. Biochem. Biotechnol.* **1996**, *57* (1), 471−480.
(32) Zhang, K.; Yang, S.-T. In situ recovery of fumaric acid by intermittent adsorption with IRA-900 ion exchange resin for enhanced fumaric acid production by Rhizopus oryzae. *Biochem. Eng. J.* **2015**, *96*, 38−45.
(33) Rebecchi, S.; Pinelli, D.; Bertin, L.; Zama, F.; Fava, F.; Frascari, D. Volatile fatty acids recovery from the effluent of an acidogenic digestion process fed with grape pomace by adsorption on ion exchange resins. *Chem. Eng. J.* **2016**, *306*, 629−639.
(34) Zhou, J.; Wu, J.; Liu, Y.; Zou, F.; Wu, J.; Li, K.; Chen, Y.; Xie, J.; Ying, H. Modeling of breakthrough curves of single and quaternary mixtures of ethanol, glucose, glycerol and acetic acid adsorption onto a microporous hyper-cross-linked resin. *Bioresour. Technol.* **2013**, *143*, 360−368.
(35) Dethe, M. J.; Marathe, K. V.; Gaikar, V. G. Adsorption of Lactic Acid on Weak Base Polymeric Resins. *Sep. Sci. Technol.* **2006**, *41* (13), 2947−2971.
(36) Qin, W.; Li, Z.; Dai, Y. Extraction of Monocarboxylic Acids with Trioctylamine: Equilibria and Correlation of Apparent Reactive Equilibrium Constant. *Ind. Eng. Chem. Res.* **2003**, *42* (24), 6196−6204.
(37) Eyal, A. M.; Canari, R. pH Dependence of Carboxylic and Mineral Acid Extraction by Amine-Based Extractants: Effects of pKa, Amine Basicity, and Diluent Properties. *Ind. Eng. Chem. Res.* **1995**, *34* (5), 1789−1798.
(38) De Haan, A. B.; Van Krieken, J.; Đekic Živkovic, T. Lactic acid extraction. WO2013/093028A1, 2013.
(39) Fu, H.; Sun, Y.; Teng, H.; Zhang, D.; Xiu, Z. Salting-out extraction of carboxylic acids. *Sep. Purif. Technol.* **2015**, *139* (0), 36−42.
(40) King, C. J.; Tung, L. A. Sorption of carboxylic acid from carboxylic salt solutions at pHs close to or above the pKa of the acid, with regeneration with an aqueous solution of ammonia or low-molecular-weight alkylamine. U.S. Patent 5132456, 1992.
(41) Tung, L. A.; King, C. J. Sorption and extraction of lactic and succinic acids at pH > pKa1. 2. Regeneration and process considerations. *Ind. Eng. Chem. Res.* **1994**, *33* (12), 3224−3229.
(42) King, C. J.; Husson, S. M. Regeneration of carboxylic acid-laden basic sorbents by leaching with a volatile base in an organic solvent. U.S. Patent 5965771, 1999.
(43) Kaufman, E. N.; Cooper, S. P.; Davison, B. H. Screening of resins for use in a biparticle fluidized-bed bioreactor for the continuous fermentation and separation of lactic acid. *Appl. Biochem. Biotechnol.* **1994**, *45* (1), 545−554.

DOI: 10.1021/acssuschemeng.7b02095
ACS Sustainable Chem. Eng. 2017, 5, 9176−9184